Institute of Experimental Morphology, Pathology and Anthropology with Museum
Bulgarian Anatomical Society

Acta Morphologica et Anthropologica, 31 (3-4)
Sofia ● 2024

ANTHROPOLOGY AND ANATOMY 31 (4)

Original Articles

Quantitative Assessment of Structural Complexity in Human Cerebellum through Analysis of Skeletonized MR Images: Anatomical Correlations, Sex Differences, and Age-Related Changes

Nataliia Maryenko, Oleksandr Stepanenko*

Department of Histology, Cytology and Embryology, Kharkiv National Medical University, Kharkiv, Ukraine

*Corresponding author e-mail: maryenko.n@gmail.com, ni.marienko@knmu.edu.ua

The present study provides a quantitative assessment of the human cerebellum structural complexity using analysis of skeletonized images. Magnetic resonance images from 100 apparently healthy individuals (aged 18-86 years) were examined. Following segmentation, the images were skeletonized, and quantitative analysis of the digital skeletons was conducted. The following parameters were determined: number of branches and their junctions, end-point, slab and junction pixels, average and maximum branch length, triple and quadruple points. Sex differences were assessed. Correlation analysis included determining the relationships between the studied parameters and age, morphometric parameters derived from Euclidean and fractal geometries, as well as the same parameters of the digital skeletons identified in the cerebral hemispheres. In conclusion, quantitative analysis of digital cerebellar skeletons offers advantages for assessing the structural complexity of the cerebellum. This method and the results of the present study can be applied in diagnosing cerebellar malformations and distinguishing between malformations and atrophic alterations.

Key words: age, cerebellum, morphometry, tomography, sex differences

Introduction

The human cerebellum possesses a complex tree-like structure characterized by the branching of its white matter. Changes in cerebellar structure, typically simplification, occur in malformations, often resembling those observed in atrophic alterations [12]. Therefore, the development of methods for quantitatively assessing cerebellar structural complexity is particularly important. Commonly used methods for quantitative characterization of the cerebellum are derived from Euclidean geometry, involving measurements of linear dimensions [4], sectional area [4, 13], and volume [15]. In recent decades, due to the fractal properties of the cerebellum (self-affinity and scale invariance), fractal analysis derived from fractal geometry has been employed to characterize cerebellar structural complexity [1, 6, 8, 16].

An alternative method used to analyze complex, tree-like structures is quantitative analysis of skeletonized images. This technique involves skeletonization of silhouette images followed by automated counting of branches, junctions, endpoints, and related parameters. It has been utilized to characterize the arborization of neuronal dendritic trees [3, 11] and glial cell processes [17]. Skeletonization can also serve as a preprocessing step for fractal analysis, including studies of neurons [5, 10], the cerebellum [6], and the white matter of the cerebral hemispheres [2, 18].

Given the tree-like nature of the cerebellar white matter and the neuron-like appearance of the cerebellum on sagittal sections, we aimed to apply quantitative analysis of skeletonized images to investigate its structural complexity. In our previous preliminary study, we employed this method for magnetic resonance (MR) images of the cerebellum as supportive analysis [8]. In the present study, we expanded the sample size from 30 to 100 and widened the age range from 18-30 years to 18-86 years. Our objective was to investigate sex differences, age-related changes, and determine the anatomical correlations of quantitative parameters of digital cerebellar skeletons.

Material and Methods

In this study, T2-weighted MR images from 100 apparently healthy individuals (44 males and 56 females), aged 18-86 years, were analyzed. The age and sex distribution of the study sample is presented in **Table 1**. Participants underwent diagnostic MR brain scanning using a 1.5 Tesla Siemens Magnetom Symphony magnetic resonance imaging scanner. Individuals with no MR confirmed brain pathology were considered ostensibly healthy and included in the study. Written informed consent was obtained from all participants. The study was approved by the Commission on Ethics and Bioethics of Kharkiv National Medical University (Minutes of Meetings No. 10 dated November 7, 2018, and No. 5 dated February 1, 2023) for research involving human subjects.

Table 1. The age and sex distribution of the participants of the study

Sex group	Age range, years				Total
	18-30	31-45	46-60	61-86	
Both, N	31	29	24	16	100
Males, N	14	14	8	8	44
Females, N	17	15	16	8	56

The midsagittal sections of the cerebellar vermis were selected for analysis (**Fig. 1A**). The image size was 160×160 pixels, with an absolute image scale of 3 pixels = 1 mm. During preprocessing, the background was removed (**Fig. 1B**), followed by segmentation using thresholding with an empirical pixel intensity threshold value of 100. This resulted in a binary silhouette image of the overall cerebellar tissue (**Fig. 1C**). Subsequently, the images underwent skeletonization using the "skeletonize" tool in Image J software [14]. The digital skeleton line thickness was set at 1 pixel (**Fig. 1D**). Skeleton analysis was conducted using the "analyze skeleton" tool in Image J (**Fig. 1E, F**). The following parameters were determined: 1. number of branches; 2. number of junctions; 3. end-point pixels (voxels) – pixels forming the

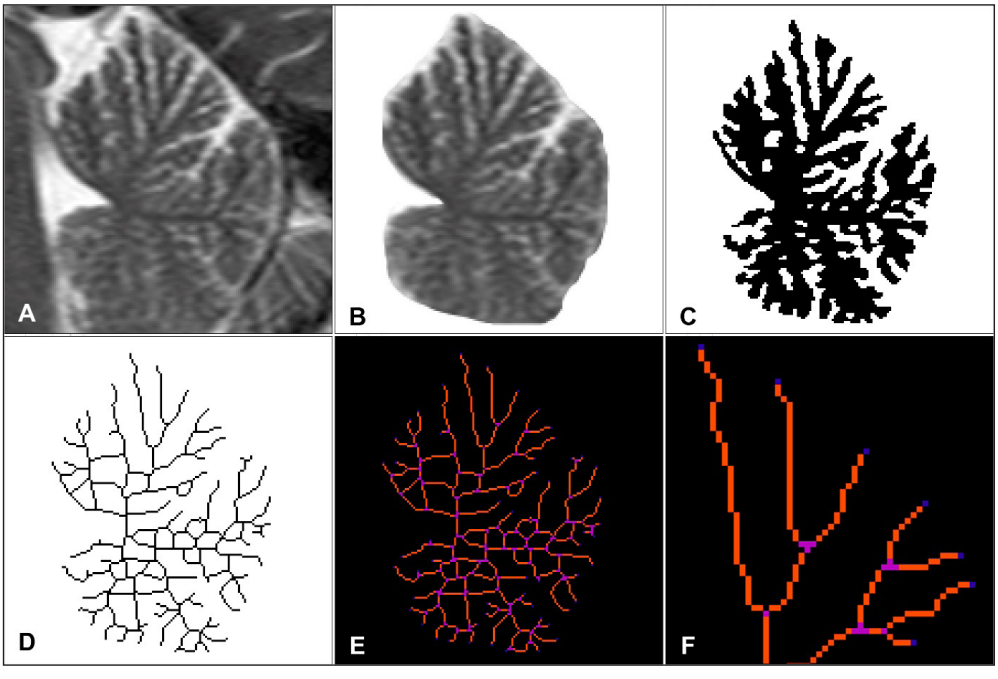

Fig. 1. Cerebellar MR image analysis algorithm (T2-weighted image, midsagittal section of the cerebellar vermis). A – initial image; B – background removal; C – segmentation of the overall cerebellar tissue; D – skeletonization; E, F – quantitative analysis of digital skeleton: slab pixels (forming branches) are shown in orange, junction pixels in purple, and end-point pixels in blue

endpoints of the digital skeleton, corresponding to the number of superficially exposed gyri; 4. junction pixels (voxels) – pixels forming the junctions; 5. slab pixels (voxels) – pixels forming the branches; 6. average branch length; 7. maximum branch length; 8. triple points (number of junctions connecting three branches); 9. quadruple points (number of junctions connecting four branches).

For correlation analysis, we used additional parameters derived from Euclidean and fractal geometries (see [9] for descriptive data and analysis of these parameters). Euclidean geometry-based parameters included: perimeter P1 (length of the visible cerebellar pial surface contour); area A1 (cerebellar tissue area, including fissures and sulci content); perimeter-to-area ratio (P1/A1); shape factor (circularity) SF1; perimeter P2 (length of the entire cerebellar pial surface contour, including hidden surface within fissures and sulci); area A2 (cerebellar tissue area excluding fissures and sulci content); perimeter-to-area ratio (P2/A2); shape factor (circularity) SF2; gyrification index calculated as P2/P1; and area ratio calculated as A2/A1. Fractal geometry-derived parameters included fractal dimensions (FD), such as FD of overall cerebellar tissue, white matter, cortex, granular layer of cortex, molecular layer of cortex, cerebellar digital skeleton, and outer contour [9].

Additionally, we examined correlation relationships between the studied parameters of cerebellar skeletons and those determined in cerebral hemispheres in our previous study (involving the same sample) [7]. The previous study analyzed five sections: four coronal and one axial, where Coronal 1 was located at the anterior poles of the temporal lobes, Coronal 2 at the level of mammillary bodies, Coronal 3 at the level of the quadrigeminal plate, Coronal 4 at the level of the splenium of the corpus callosum, and Axial at the level of the thalamus [7].

Statistical analysis was conducted using Microsoft Excel 2016. Descriptive data are presented as mean (M), standard deviation (SD), minimum value (min), 25th percentile (Q1), median (Me), 75th percentile (Q3), and maximum value (max). The normality of the value distribution was assessed using the Shapiro-Wilk W test. As some parameters exhibited non-normal distribution (**Table 2**), non-parametric statistical methods were chosen for further analysis. The Mann-Whitney U test was used to assess the significance of statistical differences between parameters in males and females. Relationships between the studied morphometric parameters were evaluated using the non-parametric Spearman's rank correlation coefficient (R), with significance determined by the Student t-test. The F-test was applied to compare linear regression equations characterizing the age dynamics of the studied parameters in males and females. The significance level for all results was set at $\alpha = 0.05$.

Results

The descriptive statistical data are presented in **Table 2**. The values of the studied parameters were distributed across a wide range. The mean and median values of most parameters (except for average and maximum branch length and quadruple points) were higher in males compared to females, but a significant difference was observed only for end-point pixels. This suggests a slightly higher branching degree in male cerebella, resulting in more numerous superficial gyri.

Table 2. Descriptive statistics for the cerebellar digital skeleton quantitative parameters

Parameter	*Sex group*	M	SD	min	Q1	Me	Q3	max	*P (normality)*	*P (sex difference)*
Branches	***Both***	114.57	25.58	48	98	114	130	178	*0.211*	*0.394*
	Males	117.27	27.18	48	98	117	131	176		
	Females	112.45	24.29	54	99	111	127	178		
Junctions	***Both***	59.52	14.16	25	51	58	67	97	*0.181*	*0.471*
	Males	60.75	14.73	25	51	62	70	95		
	Females	58.55	13.75	26	52	58	66	97		
End-point pixels	***Both***	43.29	5.36	28	40	44	47	58	*0.815*	*0.049*
	Males	44.48	6.04	28	41	45	48	58		
	Females	42.36	4.61	31	39	43	46	51		
Junction pixels	***Both***	231.74	60.51	85	194	226	262	416	*0.052*	*0.751*
	Males	234.45	62.46	85	194	226	276	379		
	Females	229.61	59.42	93	194	225	257	416		
Slab pixels	***Both***	745.8	99.03	431	679	734	816	956	*0.102*	*0.127*
	Males	758.84	96.68	431	703	762	834	908		
	Females	735.55	100.5	461	665	723	809	956		
Average branch length (pixels)	***Both***	10.77	1.01	8.88	10.11	10.65	11.43	13.44	*0.05*	*0.448*
	Males	10.71	1.17	8.88	9.94	10.37	11.6	13.44		
	Females	10.82	0.87	8.98	10.2	10.67	11.28	12.75		

CONTINUATION OF Table 2. Descriptive statistics for the cerebellar digital skeleton quantitative parameters

Parameter	*Sex group*	M	SD	min	Q1	Me	Q3	max	*P (normality)*	*P (sex difference)*
Maximum branch length (pixels)	***Both***	33.17	5.34	22.31	29.46	32.03	35.86	47.46	*0.008*	*0.767*
	Males	33.22	5.33	22.31	29.92	32.76	35.67	45.45		
	Females	33.13	5.4	24.33	29.29	31.94	36.11	47.46		
Triple points	***Both***	45.83	11.12	19	38.75	45	52	77	*0.542*	*0.464*
	Males	46.93	11.43	23	39	47	52	77		
	Females	44.96	10.9	19	37	45	52	72		
Quadruple points	***Both***	11.08	3.71	2	9	11	14	20	*0.115*	*0.876*
	Males	11.05	3.89	2	8	10	15	19		
	Females	11.11	3.6	5	9	11	13	20		

Most of the studied parameters exhibited positive correlations with each other (**Table 3**), except for average and maximum branch length, which showed negative correlations with other parameters but positive correlations with each other. This suggests that cerebella with a greater number of branches have shorter branches compared to less branched cerebella.

Table 3. Correlations of the cerebellar digital skeleton quantitative parameters

Parameter	1	2	3	4	5	6	7	8	9
	Branches	Junctions	End-point pixels	Junction pixels	Slab pixels	Average branch length	Maximum branch length	Triple points	Quadruple points
Branches	-	0.987*	0.634*	0.957*	0.805*	-0.831*	-0.291*	0.910*	0.710*
Junctions	0.987*	-	0.552*	0.938*	0.812*	-0.815*	-0.254*	0.952*	0.672*
End-point pixels	0.634*	0.552*	-	0.558*	0.475*	-0.626*	-0.236*	0.516*	0.395*
Junction pixels	0.957*	0.938*	0.558*	-	0.771*	-0.763*	-0.301*	0.827*	0.736*
Slab pixels	0.805*	0.812*	0.475*	0.771*	-	-0.390*	-0.065	0.780*	0.490*
Average branch length	-0.831*	-0.815*	-0.626*	-0.763*	-0.390*	-	0.391*	-0.765*	-0.641*
Maximum branch length	-0.291*	-0.254*	-0.236*	-0.301*	-0.065	0.391*	-	-0.178	-0.285*
Triple points	0.910*	0.952*	0.516*	0.827*	0.780*	-0.765*	-0.178	-	0.467*
Quadruple points	0.710*	0.672*	0.395*	0.736*	0.490*	-0.641*	-0.285*	0.467*	-

Note: * – $P < 0.05$

The correlation analysis with parameters derived from Euclidean geometry has shown weak to moderate correlations (**Table 4**). Specifically, most of the studied parameters characterizing branching degree (branches, junctions, end-point pixels, junction pixels, slab pixels) demonstrated positive correlations with perimeter and area values, suggesting that an increase in cerebellar vermis size results in an increase in branching degree. Additionally, the gyrification index (indirectly characterizing the number and complexity of gyri) has demonstrated positive correlations with the studied parameters, especially end-point pixels characterizing the number of superficial gyri.

Most of the studied parameters (except for maximum branch length) have shown moderate to strong correlation relationships with the parameters derived from fractal geometry (**Table 5**). The strongest correlations with quantitative parameters of the cerebellar digital skeleton were demonstrated by FD of the overall cerebellar cortex and its layers, FD of the digital skeleton, and cerebellar contour. FD of the overall

cerebellar tissue was less correlated with the studied parameters, and FD of white matter showed no significant correlations. FD is a parameter that characterizes the degree of spatial and structural complexity of the irregular figures. This explains the stronger correlations of the studied parameters with parameters of fractal geometry compared to those derived from Euclidean geometry, which best characterize structures with simple configurations.

Table 4. Correlations of the cerebellar digital skeleton quantitative parameters and Euclidean geometry derived parameters

Parameter	1	2	3	4	5	6	7	8	9
	Branches	**Junctions**	**End-point pixels**	**Junction pixels**	**Slab pixels**	**Average branch length**	**Maximum branch length**	**Triple points**	**Quadruple points**
Perimeter P1	0.383*	0.386*	0.366*	0.327*	0.644*	-0.084	0.030	0.408*	0.128
Area A1	0.338*	0.341*	0.359*	0.294*	0.626*	-0.016	0.087	0.380*	0.105
Perimeter-to-area ratio P1/A1	-0.217*	-0.215*	-0.274*	-0.194	-0.430*	-0.019	-0.079	-0.254*	-0.081
Shape factor SF1	0.002	0.004	0.033	0.024	-0.021	0.008	-0.058	0.024	0.040
Perimeter P2	0.385*	0.344*	0.612*	0.327*	0.495*	-0.238*	-0.054	0.342*	0.153
Area A2	0.355*	0.397*	0.115	0.353*	0.697*	0.048	0.106	0.465*	0.025
Perimeter-to-area ratio P2/A2	0.012	-0.053	0.387*	-0.030	-0.181	-0.211*	-0.103	-0.109	0.092
Shape factor SF2	-0.204*	-0.143	-0.557*	-0.153	-0.146	0.255*	0.110	-0.110	-0.135
Gyrification index P2/P1	0.279*	0.228*	0.558*	0.241*	0.272*	-0.253*	-0.089	0.209*	0.148
Area ratio A2/A1	0.153	0.209*	-0.225*	0.190	0.349*	0.082	0.032	0.259*	-0.064

Note: * – $P < 0.05$

Table 5. Correlations of the cerebellar digital skeleton quantitative parameters and fractal geometry derived parameters

Parameter	1	2	3	4	5	6	7	8	9
	Branches	Junctions	End-point pixels	Junction pixels	Slab pixels	Average branch length	Maximum branch length	Triple points	Quadruple points
FD(overall tissue)	0.448*	0.442*	0.266*	0.438*	0.480*	-0.287*	-0.094	0.414*	0.266*
FD (white matter)	-0.079	-0.066	-0.045	-0.069	-0.059	0.037	-0.010	-0.055	-0.073
FD (overall cortex)	0.642*	0.617*	0.455*	0.608*	0.565*	-0.494*	-0.151	0.572*	0.441*
FD (granular layer of cortex)	0.651*	0.634*	0.384*	0.633*	0.633*	-0.463*	-0.142	0.591*	0.465*
FD (molecular layer of cortex)	0.620*	0.595*	0.435*	0.571*	0.536*	-0.502*	-0.179	0.552*	0.443*
FD (skeleton)	0.801*	0.772*	0.494*	0.775*	0.681*	-0.615*	-0.240*	0.693*	0.563*
FD (contour)	0.553*	0.540*	0.402*	0.488*	0.587*	-0.376*	-0.104	0.518*	0.313*

Note: * – $P < 0.05$

The parameters of the cerebellar skeletons have shown mostly weak correlations with the same parameters determined in the cerebral hemispheres (**Table 6**). Moderate significant correlations were shown by slab pixels and end-point pixels, which characterize the number of gyri in both the cerebellum and cerebrum. It can be assumed that there are common factors leading to the complication of the configuration of both brain regions.

Table 6. Correlations of the cerebellar digital skeleton quantitative parameters with the same parameters determined in cerebral hemispheres

Parameter	1	2	3	4	5	6	7	8	9
Section of cerebral hemispheres	**Branches**	**Junctions**	**End-point pixels**	**Junction pixels**	**Slab pixels**	**Average branch length**	**Maximum branch length**	**Triple points**	**Quadruple points**
Coronal 1	0.236*	0.266*	0.075	0.162	0.350*	-0.144	-0.161	0.083	0.161
Coronal 2	0.249*	0.230*	0.225*	0.185	0.268*	-0.292*	-0.056	0.052	-0.160
Coronal 3	0.228*	0.210*	0.324*	0.129	0.351*	-0.195	0.020	-0.164	-0.052
Coronal 4	0.233*	0.226*	0.201*	0.203*	0.219*	-0.238*	0.103	-0.041	-0.088
Axial	-0.001	-0.006	0.124	-0.017	0.123	-0.075	0.031	0.022	0.061
Average value (all sections)	0.268*	0.239*	0.309*	0.203*	0.345*	-0.276*	0.007	-0.019	-0.030

Note: * – $P < 0.05$

The correlations with age were mostly weak (**Table 7**). The parameters characterizing the branching degree showed slight decreases during aging.

Table 7. Correlations of the cerebellar digital skeleton quantitative parameters and age

Sex group	**Parameter**	**1**	**2**	**3**	**4**	**5**	**6**	**7**	**8**	**9**
		Branches	**Junctions**	**End-point pixels**	**Junction pixels**	**Slab pixels**	**Average branch length**	**Maximum branch length**	**Triple points**	**Quadruple points**
Both	**R**	-0.364*	-0.350*	-0.249*	-0.336*	-0.379*	0.227*	0.035	-0.348*	-0.223*
	Rn(A1)	-0.261*	-0.244*	-0.119	-0.247*	-0.170	0.242*	0.078	-0.227*	-0.198*
Males	**R**	-0.390*	-0.394*	-0.282	-0.348*	-0.449*	0.222	0.000	-0.430*	-0.150
	Rn(A1)	-0.282	-0.294	-0.081	-0.240	-0.207	0.228	-0.013	-0.329*	-0.134
Females	**R**	-0.317*	-0.287*	-0.204	-0.307*	-0.307*	0.210	0.082	-0.277*	-0.248
	Rn(A1)	-0.214	-0.172	-0.132	-0.225	-0.110	0.240	0.160	-0.143	-0.207

Note: * – $P < 0.05$; R – regular correlation coefficient; Rn(A1) – correlation coefficient normalized by area A1

Considering the positive correlations of the studied parameters with the absolute sizes of the cerebellum, we computed correlation coefficients normalized by area A1 (**Table 7**). The normalized correlations were weaker, supporting the suggestion of the area's influence. After normalization, the end-point pixels showed no significant correlations with age. The correlations of the studied parameters with age in males were slightly stronger than in females, but after area normalization, only a few correlations remained significant. Comparing linear regression equations characterizing the age dynamics in males and females, no significant differences were observed ($P > 0.05$).

Discussion

The present study employed quantitative analysis of skeletonized images of the cerebellum – a method commonly used for investigating neurons and the branched processes of glial cells [3, 11, 17]. Considering the tree-like configuration of the cerebellum, this method has proven informative not only at the microscopic but also at the macroscopic level of brain organization. Quantitative analysis of the digital skeleton allows for a quantitative and automated characterization of the structural complexity of tree-like structures: the more gyri the cerebellum has and the higher its branching degree, the higher the degree of structural complexity, resulting in a digital skeleton with more branches, junctions, and endpoints.

A prospective application of the results of the present study is in the diagnosis of malformations and their differentiation from atrophic changes. For this purpose, it is necessary to select a parameter that remains unchanged or changes minimally throughout life. Such a parameter can be considered the number of endpoint pixels (the number of gyri remains constant throughout life). It can be assumed that in atrophic alterations, this parameter will remain unchanged, while in malformations, significant changes in all parameters characterizing the structural complexity of the cerebellum may be observed. The FD values, which also characterize the structural complexity, are often affected by age-related changes of brain [2, 9, 18]. Therefore, the parameters of digital skeletons are more appropriate for this purpose.

Conclusions

Quantitative analysis of skeletonized images is an informative method of investigation for complex tree-like structures and can be applied not only at the microscopic but also at the macroscopic level. This method can be used in clinical practice for diagnosing cerebellar malformations and in theoretical neuromorphological studies to characterize the structural complexity of the cerebellum and other brain structures.

References

1. **Akar, E., S. Kara, H. Akdemir, A. Kırış.** 3D structural complexity analysis of cerebellum in Chiari malformation type I. – *Medical & Biological Engineering & Computing*, **55**(12), 2017, 2169-2182.
2. **Farahibozorg, S., M. Hashemi-Golpayegani, J. Ashburner.** Age- and sex-related variations in the brain white matter fractal dimension throughout adulthood: an MRI study. – *Clinical Neuroradiology*, **25**(1), 2015, 19-32.
3. **Greenblum, A., R. Sznitman, P. Fua, E. Arratia, M. Oren, B. Podbilewicz, J. Sznitman.** Dendritic tree extraction from noisy maximum intensity projection images in C. elegans. – *Biomedical Engineering Online,* **13**, 2014, 74.
4. **Hayakawa, K., Y. Konishi, T. Matsuda, M. Kuriyama, K. Konishi, K. Yamashita, R. Okumura, D. Hamanaka.** Development and aging of brain midline structures: assessment with MR imaging. – *Radiology*, **172**(1), 1989, 171–177.
5. **Jelinek, H. F., E. Fernandez.** Neurons and fractals: how reliable and useful are calculations of fractal dimensions? – *Journal of Neuroscience Methods*, **81**(1-2), 1998, 9-18.
6. **Liu, J. Z., L. D. Zhang, G. H. Yue.** Fractal dimension in human cerebellum measured by magnetic resonance imaging. – *Biophysical Journal*, **85**(6), 2003, 4041-4046.
7. **Maryenko, N. I., O. Y. Stepanenko.** Shape of cerebral hemispheres: structural and spatial complexity. Quantitative analysis of skeletonized MR images. – *Reports of Morphology*, **28**(3), 2022, 62-73.
8. **Maryenko, N., O. Stepanenko.** Characterization of white matter branching in human cerebella: quantitative morphological assessment and fractal analysis of skeletonized MR images. – *Biomedical Research and Therapy*, **8**(5), 2021, 4345-4357.
9. **Maryenko, N. I., O. Y. Stepanenko.** Evaluation of cerebellar aging in MRI images: Fractal analysis compared to Euclidean geometry-based morphometry. – *Meta-Radiology*, **2**(3), 2024, 100101(1-12).
10. **Milosević, N. T., D. Ristanović.** Fractality of dendritic arborization of spinal cord neurons. – *Neurosci. Lett*, **396**(3), 2006, 172-176.
11. **Orlowski, D., C. R. Bjarkam.** A simple reproducible and time saving method of semi-automatic dendrite spine density estimation compared to manual spine counting. – *J. Neurosci. Methods*, 208(2), 2012, 128-133.
12. **Poretti, A., E. Boltshauser, D. Doherty.** Cerebellar hypoplasia: Differential diagnosis and diagnostic approach. – *Am. J. Med. Genet. Part C Semin. Med. Genet*., **166**, 2014, 211-226.
13. **Raz, N., I. J. Torres, W. D. Spencer, K. White, J. D. Acker.** Age-related regional differences in cerebellar vermis observed in vivo. – *Archives of Neurology*, **49**(4), 1992, 412–416.
14. **Schneider, C. A., W. S. Rasband, K. W. Eliceiri.** NIH Image to ImageJ: 25 years of image analysis. – *Nature Methods*, **9**(7), 2012, 671-675.
15. **Serati, M., G. Delvecchio, G. Orsenigo, C. Perlini, M. Barillari, M. Ruggeri, A. C. Altamura, M. Bellani, P. Brambilla.** Potential gender-related aging processes occur earlier and faster in the vermis of patients with bipolar disorder: An MRI study. – *Neuropsychobiology*, 75(1), 2017, 32-38.

16. **Wu, Y. T., K. K. Shyu, C. W. Jao, Z. Y. Wang, B. W. Soong, H. M. Wu, P. S. Wang.** Fractal dimension analysis for quantifying cerebellar morphological change of multiple system atrophy of the cerebellar type (MSA-C). – *NeuroImage*, **49**(1), 2010, 539–551.
17. **Young, K., H. Morrison.** Quantifying microglia morphology from photomicrographs of immunohistochemistry prepared tissue using ImageJ. – *Journal of Visualized Experiments*, **136**, 2018, 5764.
18. **Zhang, L., D. Dean, J. Z. Liu, V. Sahgal, X. Wang, X., G. H. Yue.** Quantifying degeneration of white matter in normal aging using fractal dimension. – *Neurobiology of Aging*, **28**(10), 2007, 1543-1555.